APPROPRIATE TECHNOLOGIES TO COMBAT WATER POLLUTION

CrossMark

Degradation of naproxen in chlorination and UV/chlorine processes: kinetics and degradation products

Yongze Liu[1] · Yuqing Tang[1] · Yongxin Wu[1] · Li Feng[1] · Liqiu Zhang[1]

Abstract
Naproxen (NAP) is a nonsteroidal anti-inflammatory drug which has been widely used and frequently detected in water environments. This study investigated the NAP degradation in the chlorination and UV/chlorine disinfection processes, which usually acted as the last barriers for water treatment. The results showed that both chlorination and UV/chlorine disinfection could remove NAP effectively. At various chlorine dosages (0.1~0.5 mM), the contributions of chlorination and reactive radicals to the degradation of NAP in the UV/chlorine process were calculated to be 50.5~56.9% and 43.1~49.5%, respectively. However, the reactive radicals dominated in NAP degradation in alkaline solutions, while chlorination dominated in acidic conditions. The HCO_3^- (10~50 mM) slightly inhibited, Cl^- (10~50 mM) gradually promoted, and HA (1~5 mg/L) significantly reduced NAP degradation by UV/chlorine process. The degradation intermediates and products were obtained via high-performance liquid chromatography with QE-MS/MS; NAP was degraded by demethylation, acetylation, and dicarboxylic acid pathways during the chlorination and UV/chlorination processes.
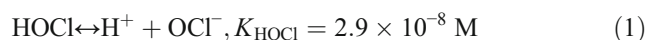
Keywords Naproxen · Chlorination · UV/chlorine disinfection · Kinetics · Degradation products

Introduction

Pharmaceutical and personal care products (PPCPs), which were widely used, have been frequently detected in aquatic environments all over the world (Vieno et al. 2007). Many of them are continuously discharged into the ecosystems, raising potential environmental threat risk to human health and ecosystems (Christen et al. 2010). Naproxen (NAP) is a nonsteroidal anti-inflammatory drug (NSAID), which is widely used to treat rheumatoid arthritis due to its antipyretic and analgesic characteristics (Alexander 1975). It can also be used frequently for livestock with up to 9 tons of prescriptions per year (Sirés and Brillas 2012). It was reported that the exposure concentration of NAP in natural waters was between 0.03 and 1.5 μg L^{-1} (Sirés and Brillas 2012; Stumpf et al. 1999;

Fernández et al. 2010). In wastewater treatment plants (WWTPs) influent, 11 μg L^{-1} NAP was detected (Santos et al. 2005). NAP still eluted at 0.25–5.2 μg L^{-1} concentrations after major biological treatment (Bendz et al. 2005; Rosal et al. 2010; Tixier et al. 2003). The occurrence of NAP in waterbodies comes from improper disposal as well as through human and animal excretion. NAP was difficult to be removed in WWTPs; thus, it became persistent pollutant in waterbodies.
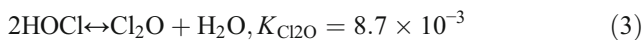
Several methods such as activated carbon adsorption, photocatalytic process, ozonation, and advanced oxidation processes have been investigated to better remove NAP from water environments (Luo et al. 2014; Štrbac et al. 2018). Disinfection process is the last barrier in the water treatment process and it plays an important role in the removal of PPCPs. As the earliest chemical disinfectant used for disinfection of water, free chlorine has been one of the main technical methods for water disinfection in various countries all over the world. Chlorine is hydrolyzed and dissociated in water producing HOCl, ClO⁻, Cl₂, and Cl₂O (Eqs. 1–3) (von Gunten 2003; Morris 1966; Cai et al. 2013, 2017; Wang and Margerum 2002; Deborde and von Gunten 2008).
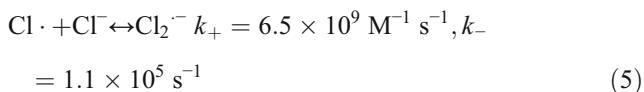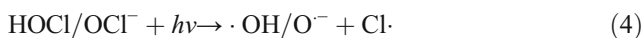
$$HOCl \leftrightarrow H^+ + OCl^-, K_{HOCl} = 2.9 \times 10^{-8} \text{ M} \tag{1}$$

$$Cl_2 + H_2O \leftrightarrow HOCl + H^+ + Cl^-, K_{Cl2} = 5.1 \times 10^{-4} \text{ M}^2 \quad (2)$$

$$2HOCl \leftrightarrow Cl_2O + H_2O, K_{Cl2O} = 8.7 \times 10^{-3} \quad (3)$$

Ultraviolet (UV) photolysis is a physical process that has no residual and sustained disinfection capacity compared to chlorination (Hijnen et al. 2006). Therefore, UV disinfection and other disinfection processes are always used in combination. The UV/chlorine disinfection process can kill the protozoa making up the defect of chlorination and also reduce the water quality toxicity of the water body. On the other hand, synergistic effects of UV and chlorine disinfection can also reduce the dosage of disinfectants and the production of disinfection byproducts (DBPs) in water, and further ensuring the safety of water. Compared with traditional chlorination disinfection process, UV/chlorine cannot only inactivate waterborne pathogenic microorganisms but also destroy harmful organic compounds produced in water treatment processes (Deng et al. 2013; Hijnen et al. 2006). During UV/chlorine process, hydroxyl radicals (HO·), and reactive chlorine radicals (RCS, such as Cl·/Cl$_2$·$^-$) were generated via UV photolysis of HOCl/OCl$^-$ (Eqs. 4–5) (Fang et al. 2014).

$$HOCl/OCl^- + h\nu \rightarrow \cdot OH/O^{\cdot -} + Cl\cdot \quad (4)$$

$$Cl \cdot + Cl^- \leftrightarrow Cl_2^{\cdot -} \quad k_+ = 6.5 \times 10^9 \text{ M}^{-1} \text{ s}^{-1}, k_-$$
$$= 1.1 \times 10^5 \text{ s}^{-1} \quad (5)$$

Previous studies only focused on the degradation kinetics of NAP (Boyd et al. 2005). However, little attention was paid to the formation of active components (such as OH·, RCS, HOCl, and OCl$^-$). This study expounded the NAP degradation kinetics and pathways in UV/chlorine process via the following steps: (i) comparing the degradation of NAP between dark chlorination and UV/chlorination and examining the degradation kinetics at different chlorine dosages; (ii) assessing effects of pH on the degradation of NAP and calculating relative contributions of different processes (such as chlorination, radicals oxidation) to the degradation of NAP; (iii) elucidating the effects of water matrices (such as chloride ion (Cl$^-$), bicarbonates (HCO$_3^-$), and humic acid (HA)) on NAP degradation; (iv) detecting the degradation intermediates and products of NAP and proposing the corresponding degradation pathways.

Materials and methods

Materials

NAP (> 98%) and sodium hypochlorite (OCl$^-$) containing 8% available free chlorine were purchased from J&K Scientific,

Ltd. (China) and used without purification. NaOH, HClO$_4$, NaCl, NaHCO$_3$, and KH$_2$PO$_4$ were of analytical grade or above and were purchased from Xilong Chemical Co., Ltd. (China). N, N-diethyl-p-phenylenediamine (DPD, > 99%) was obtained from Sigma-Aldrich. All solutions were dissolved in Milli-Q water generated from Millipore System. The NAP stock solution (100 μM) was prepared by dissolving 23.026 mg NAP powder into 1 L Milli-Q water, and the solution was continuously stirred using a magnetic stirrer for 2 weeks until the NAP powder was completely dissolved. Then, the NAP stock solution was stored at 4 °C in brown bottle to avoid light.

UV photolysis device

The UV light used in the experiment was generated by a collimated beam device with four low-pressure mercury UV lamps (Heraeus, GPH 212T5L/4, 254 nm, 10 W) (Yang et al. 2014). A cylindrical glass reactor (5.65 cm inner diameter and 4 cm height) containing 100-mL solution was placed 30 cm under the UV lamps, rapidly mixed at 400 rpm by the magnitude stirrer. The average surface light intensity of UV lamps was 0.16 mW cm^{-2} measured by a UV-254 radiometer (Photoelectric Instrument Factory of Beijing Normal University, China) (Watts and Linden 2007).

Experimental procedures

The photo-reactor contained an initial NAP concentration (10 μM) and phosphate buffer (0.5 mM). The initial NAP concentration 10 μM (i.e., 2.3 mg/L) in the experimental procedures was higher than that found the real water system due to the difficulty to reveal the reaction mechanism at low concentration. The specific amount of OCl$^-$ stock solution was added into the photo-reactor to initiate the reaction. Control experiments were performed in UV irradiation alone and chlorination alone. The pH of the buffer solution was adjusted via NaOH (1 mM) and HClO$_4$ (1 mM). Samples of 1.5 mL were taken at regular intervals and immediately quenched with excess ascorbic acid solution (1 M). The samples were stored in the dark at 4 °C until analysis. All the tests were conducted in triplicate and the data in average and the standard deviations were shown. Especially, higher initial concentrations of NAP (0.1 mM) and chlorine (1.0 mM) were conducted for better analysis of degradation intermediates and pathways.

Analytical methods

The DPD colorimetric method was used to determine the concentrations of free chlorine (Fang et al. 2014). The NAP concentrations were analyzed through high-performance liquid chromatography system (HPLC) (Agilent 1260 series, USA) equipped with a UV detector and a Poroshell 120 EC-C18 column (4.6 × 50 mm, 2.7 mm, Agilent, USA). The injection

volume of sample was 10 μL. The flow rate of mobile phase was 1 mL/min, and the composition of the mobile phase was 0.01% acetic acid/methanol/acetonitrile ($v/v/v$ = 40:5:55). The column temperature was maintained at 30 °C and the detected wavelength was set at 231 nm. The NAP degradation intermediates and products were identified by high-performance liquid chromatography (Ultimate 3000, Thermo Scientific, USA) with QE-MS/MS (QExactive plus, Thermo Scientific, USA). The C18 column (2.1 mm × 100 mm, 1.7 μm, Waters, China) was used as separation column. The mobile phase consisted of pure water (A) and acetonitrile (B), eluting according to the following gradient pattern: 0–8.0 min, 85% A and 15% B; 8.0–20.0 min, A decreased linearly from 85 to 20%; while B increased from 15 to 80%; 20.0–35.0 min, A increased linearly from 20 to 85%, while B decreased from 80 to 15%; 35.0–45.0 min, A and B maintained at 85% and 15%, respectively. The flow rate of mobile phase was 0.2 mL/min.

Toxicity measurement

The genetic toxicity was measured by micronucleus test of Viciafaba root tip. According to the previous report (Jia et al. 2018), the test procedure was divided into four steps. (1) germination, soaking the Viciafabas in Milli-Q water for 24 h, then culturing these Viciafabas with wet gauze overlay for another 48 h. (2) Contamination, dividing the Viciafabas with length of emerging roots 1–2 cm into four groups. Among them, two groups were contaminated by chlorination-degraded NAP and UV/chlorine-degraded NAP for 12 h, respectively, one group was contaminated by 0.05 mM NAP solution for 12 h as blank control groups, and one group was treated by Milli-Q water for 12 h as negative control group. (3) Disaggregation, culturing four groups in Milli-Q water for 24 h after contamination for recovery, then cutting 1 cm root tips and fixing in Carnoy's fluid for 12 h, then disaggregating with 5 M HCl solution at 28 °C for 30 min. (4) Microscopic examination, cutting the mitotic zones (1 mm) of the disaggregated root tips and pressing them into thin lamina, dripping few drops of Schiff's reagent for dyeing 30 min in dark, then identifying by microscope (B204, Aote, China).

Results and discussion

NAP degradation in UV photolysis, dark chlorination, and UV/chlorine processes

The degradation of NAP in dark chlorination, UV irradiation, and UV/chlorine processes are shown in Fig. 1. It was found that NAP was hardly degraded under only UV photolysis, while degraded efficiently both in dark chlorination and UV/chlorine processes at 0.1 mM dosage of chlorine. The NAP
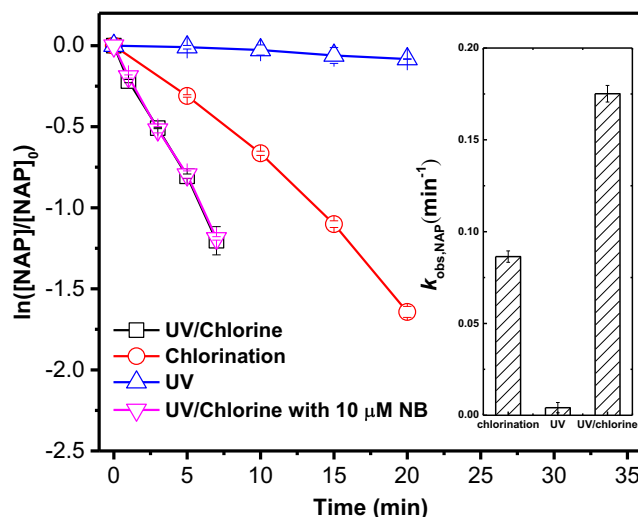

Fig. 1 NAP degradation during UV photolysis, chlorination, and UV/chlorine process. Experimental conditions: I_0 = 0.16 mW cm^{-2}, [chlorine]$_0$ = 0.1 mM, [NAP]$_0$ = 10 μM, pH = 7.0, T = 20 °C

degradation followed first-order kinetics, and the observed rate constants during dark chlorination ($k_{obs,chlorination}$) and UV/chlorine processes ($k_{obs,NAP}$) were obtained to be 0.0864 and 0.1751 min^{-1}, respectively (Fig. 1 inset). It suggested that combination of UV irradiation with chlorination enhanced NAP degradation greatly. As mentioned above, reactive radicals were generated via photolysis of free chlorine (Eqs. 4–5) (Fang et al. 2014). Therefore, the enhanced degradation rate of NAP could be attributed to the formation of reactive radicals during UV/chlorine process.

The NAP degradation in UV/chlorine process corresponded with Eqs. (6)–(7) (Guo et al. 2016).

$$-d[NAP]/dt = k_{obs,NAP}[NAP]$$
$$= k_{obs,radicals}[NAP] + k_{obs,chlorination}[NAP] + k_{obs,UV}[NAP] \tag{6}$$

$$k_{obs,NAP} = k_{obs,radicals} + k_{obs,chlorination} + k_{obs,UV} \tag{7}$$

where [NAP] represents the concentration of NAP in the reaction system at time t, $k_{obs,radicals}$, $k_{obs,chlorination}$, and $k_{obs,UV}$ stand for the observed first-order rate constants of NAP degradation by the reactive radicals, chlorination, and UV photolysis, respectively. The $k_{obs,chlorination}$ could be obtained via NAP degradation in dark chlorination process. In both dark chlorination and UV/chlorine processes, the consumptions of chlorine were relatively low, within the 20% of initial chlorine dosages. Thus, the $k_{obs,chlorination}$ obtained in UV/chlorine processes was similar with that $k_{obs,chlorination}$ obtained in dark chlorination process. The discrepancy was within 20%. The direct photolysis of NAP was negligible (as shown above), so the $k_{obs,radicals}$ could be calculated by Eq. (7). Thus, the contributions of chlorination and reactive radical oxidation

(including RCS and OH·) to NAP degradation in UV/chlorine process could be given.

Based on the obtained $k_{obs,NAP}$, the contributions of chlorination and reactive radicals to NAP degradation at 0.1 mM chlorine dosage could be calculated to be 50.5% and 49.5%, respectively. During UV/chlorine process, OH· and reactive chlorine radicals (RCS, such as Cl·/Cl$_2^{\cdot-}$) were the main reactive radicals. To distinguish the dominant reactive radicals in NAP degradation in UV/chlorine process, nitrobenzene (NB) was selected to quench OH· (Tang et al. 2018). The rate constants of NB ($k_{OH·,NB}$) and NAP ($k_{OH·,NAP}$) with OH· are 3×10^9 M^{-1} s^{-1} and 4.32×10^9 M^{-1} s^{-1} (Luo et al. 2018), respectively. By applying these constants, 10 μM NB should compete at least 40% of OH· for NAP (10 μM) degradation (i.e., $k_{OH·,NB}[NB]/(k_{OH·,NB}[NB] + k_{OH·,NAP}[NAP])$). However, with the addition of 10 μM NB, there was no obvious suppression of NAP degradation (as shown in Fig. 1), indicating little contribution of HO· to the NAP degradation. Thus, the RCS oxidation is the dominant reaction pathway in UV/chlorine process.

Effects of chlorine dosage on NAP degradation in dark chlorination and UV/chlorine processes

Figure 2 reveals the effects of chlorine dosages ([chlorine]$_0$, 0.1–0.5 mM) on NAP degradation in dark chlorination and UV/chlorine processes. Consistently, the NAP degradation at

various chlorine dosages followed first-order kinetics and the $k_{obs,NAP}$ were obtained. As shown in Fig. 2, the $k_{obs,chlorination}$ in dark chlorination increased linearly from 0.0864 to 0.6423 min^{-1} with increasing from 0.1 to 0.5 mM of chlorine dosage. Similarly, when chlorine dosage increased from 0.1 to 0.5 mM, the $k_{obs,NAP}$ increased linearly from 0.1751 to 1.2654 min^{-1}. Under UV irradiation, increasing chlorine dosage resulted in the increase of free radical production, accelerating NAP degradation rate. Based on the obtained $k_{obs,NAP}$ at different chlorine dosages, the contributions of reactive radicals and chlorination to the degradation of NAP were calculated to be 43.1~49.5% and 50.5~56.9% (Table 1), respectively. The relative contributions of these two processes changed slightly at various chlorine dosages.

Effect of pH on the degradation of NAP in dark chlorination and UV/chlorine processes

Figure 3 showed the degradation efficiencies of NAP in dark chlorination and UV/chlorine processes at the range of pH from 5 to 10. As shown, with the decrease of pH, the $k_{obs,chlorination}$ of dark chlorination increased significantly. This could be explained by the different reactivity of chlorine species with non-ionized (NAP) and ionized forms (NAP$^-$) of NAP. The intrinsic rate constants of HOCl with NAP, HOCl with NAP$^-$, and acid-catalyzed HOCl oxidation of NAP have been reported to be 300 ± 60, 9 ± 3 M^{-1} s^{-1}, and $(1.1 \pm 0.2) \times$

Fig. 2 The degradation kinetics of NAP at different chlorine dosages in chlorination and UV/chlorine process. Experimental conditions: I$_0$ = 0.16 mW cm^{-2}, [NAP]$_0$ = 10 μM, pH = 7.0, T = 20 °C
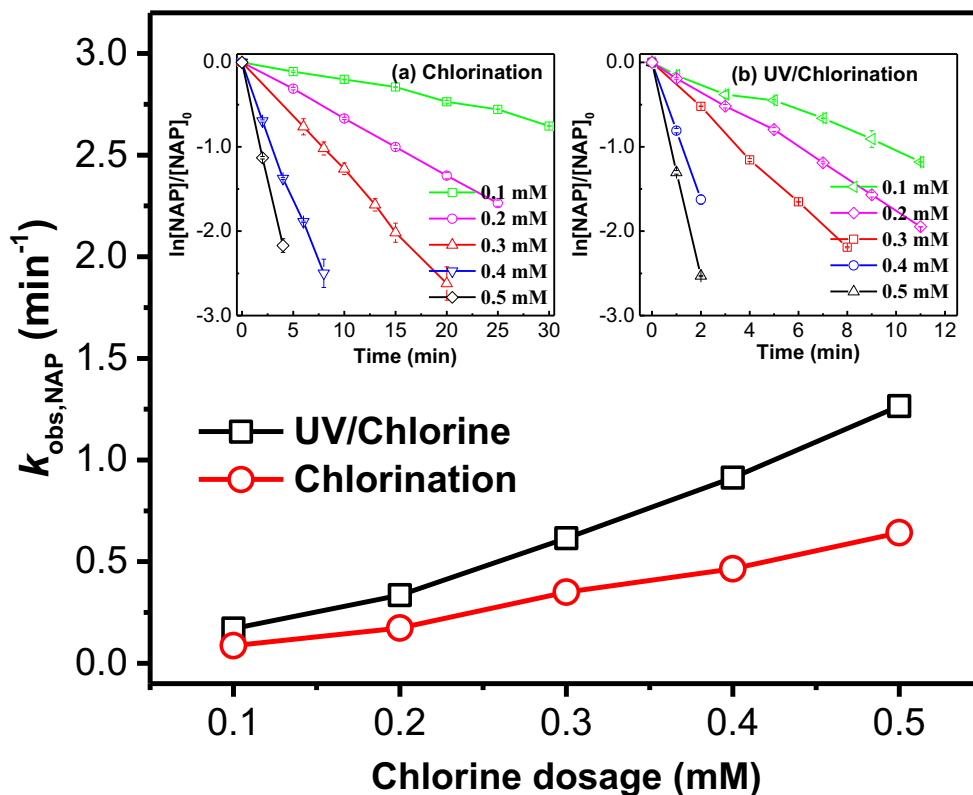
Table 1 The contributions of chlorination and reactive radicals to NAP degradation at different chlorine dosages and pH

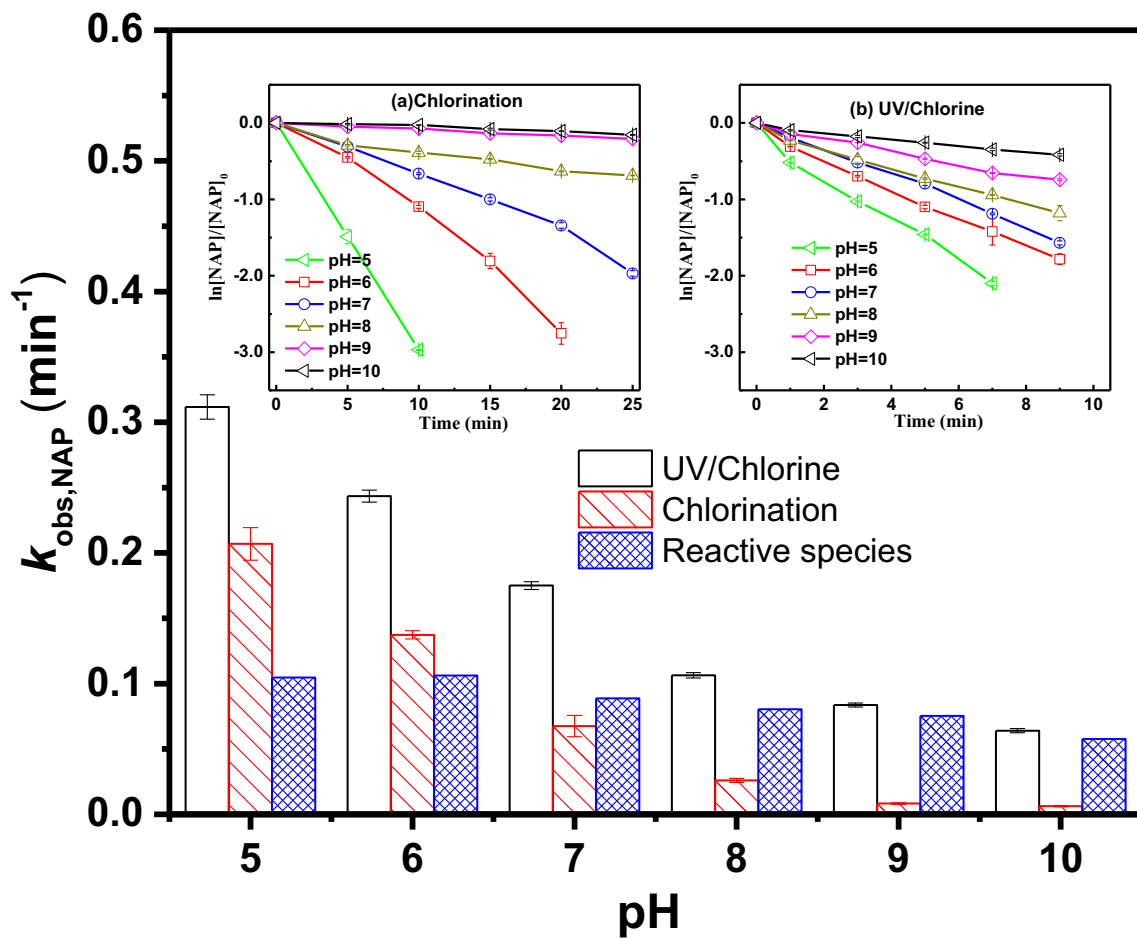|	Dark chlorination		UV/chlorine	
	$k_{obs, NAP}$ (min^{-1})	Contributions of chlorination	$k_{obs, NAP}$ (min^{-1})	Contributions of reactive radicals
[Chlorine]$_0$	pH = 7.0			
0.1 mM	0.0864	50.5%	0.1751	49.5%
0.2 mM	0.1740	51.9%	0.3351	48.1%
0.3 mM	0.3500	56.9%	0.6156	43.1%
0.4 mM	0.4650	50.9%	0.9127	49.1%
0.5 mM	0.6423	50.8%	1.2654	49.2%
pH	[Chlorine]$_0$ = 0.1 mM			
5	0.207	66.4%	0.3117	33.6%
6	0.1373	56.4%	0.2435	43.6%
7	0.0864	50.5%	0.1751	49.5%
8	0.026	20.6%	0.1264	79.4%
9	0.0083	9.9%	0.0836	90.1%
10	0.0063	9.8%	0.064	90.1%

Fig. 3 The degradation kinetics of NAP at different pH in chlorination and UV/chlorine disinfection processes. Experimental conditions: I$_0$ = 0.16 mW cm^{-2}, [chlorine]$_0$ = 0.1 mM, [NAP]$_0$ = 10 μM, T = 20 °C
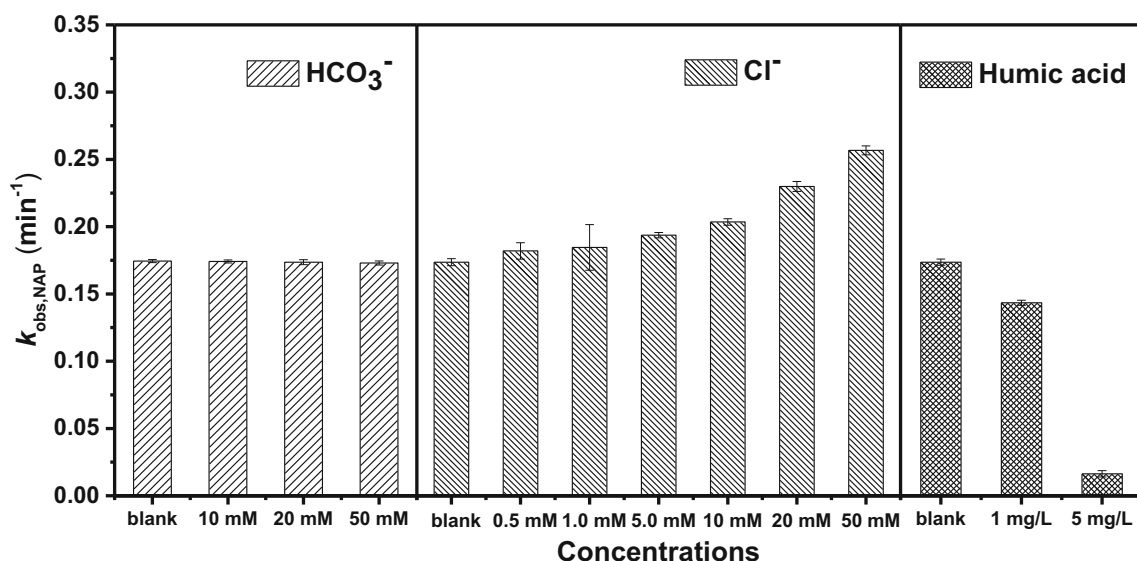
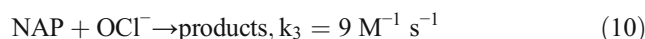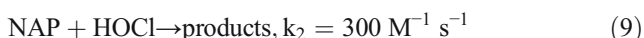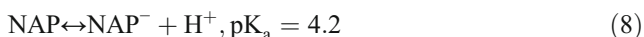**Fig. 4** Effect of water matrices (chloride, bicarbonate, and humic acid) on NAP degradation in UV/chlorine process. Experimental conditions: $I_0 = 0.16$ mW cm^{-2}, $[chlorine]_0 = 0.1$ mM, $[NAP]_0 = 10$ μM, pH = 7.0, T = 20 °C

10^6 M^{-1} s^{-1}, respectively (i.e., reactions 8–11) (Acero et al. 2010). The reactivity of OCl$^-$ with NAP is low and could be negligible compared to HOCl (Deborde and von Gunten 2008). Given that the pKa of NAP is 4.2, with the decrease of pH from 10 to 5, the concentration of NAP increased dramatically and the concentration of NAP$^-$ decreased. Thus, the decrease of pH resulting in the increase of $k_{obs,chlorination}$.

$$NAP \leftrightarrow NAP^- + H^+, pK_a = 4.2 \tag{8}$$

$$NAP + HOCl \rightarrow products, k_2 = 300 \text{ M}^{-1} \text{ s}^{-1} \tag{9}$$

$$NAP + OCl^- \rightarrow products, k_3 = 9 \text{ M}^{-1} \text{ s}^{-1} \tag{10}$$

$$NAP + HOCl + H^+ \rightarrow products, k_4$$
$$= 1.1 \times 10^6 \text{ M}^{-1} \text{ s}^{-1} \tag{11}$$
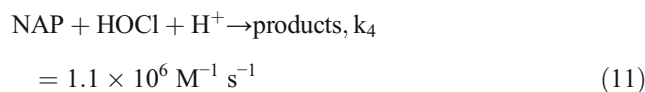
In the UV/chlorine process, the degradation rate of NAP was higher under acidic conditions and decreased at alkaline conditions (Fig. 3). As descried by Eq. (7), in UV/chlorine process, both chlorination and reactive species formed via UV photolysis of chlorine contributed to NAP degradation.

Fig. 5 Extracted total ion chromatogram (TIC) of NAP degradation in UV/chlorine process. Experimental conditions: $I_0 = 0.16$ mW cm^{-2}, $[NAP]_0 = 0.1$ mM, $[chlorine]_0 = 0.5$ mM, pH = 7.0, T = 20 °C
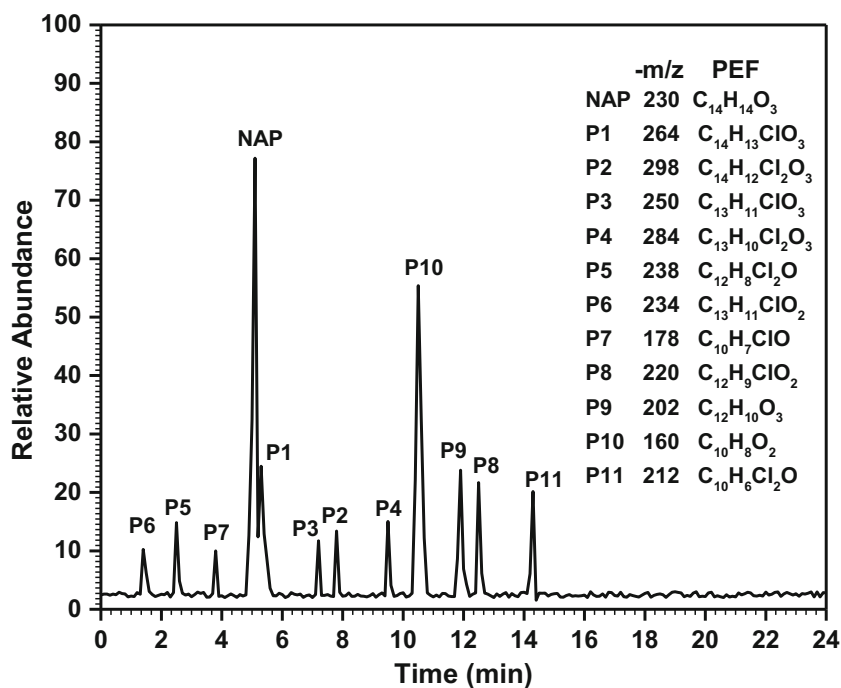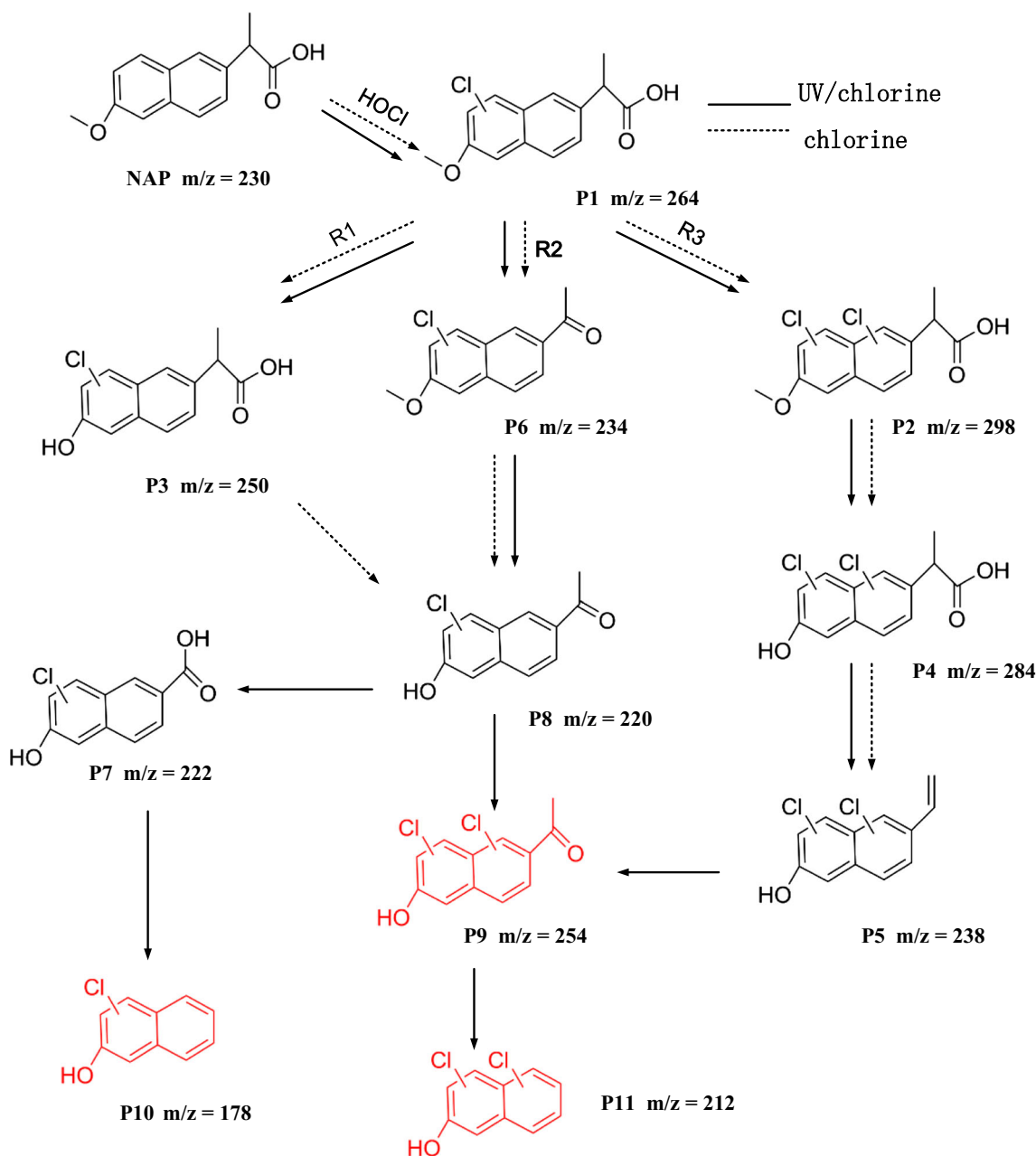
Fig. 6 The degradation pathways of NAP in chlorination (dotted line) and UV/chlorine processes (solid line). Experimental conditions: $I_0 = 0.16$ mW cm^{-2}, [NAP]$_0 = 0.1$ mM, and [chlorine]$_0 = 0.5$ mM, pH = 7.0, T = 20 °C

From Fig. 3, it could be obtained that in UV/chlorine process, chlorination was dominant in NAP degradation under acid conditions (pH < 6), while reactive radicals played the leading role under alkaline conditions (pH > 8), as given in Table 1.

Besides the effect of pH on the NAP chlorination process (as discussed above), the pH also affected the NAP degradation by reactive species. As shown in Fig. 3, with the increase of pH from 5 to 10, the NAP degradation via reactive species (i.e., $k_{obs,NAP}$-$k_{obs,chlorination}$) decreased slightly from 0.1047 to 0.0577 min^{-1}. This pH effect on reactive species was similar to the degradation of chloramphenicol in UV/chlorine process as reported previously

(Dong et al. 2017) and could be ascribed to two reasons. The pKa of HOCl/OCl$^-$ is 7.5; thus, HOCl is the main specie at low pH, whereas OCl$^-$ dominates in the speciation at high pH. The quantum yield of HOCl is 1.45, which means that 1.45 mol radicals (i.e., HO· and reactive chlorine species) are produced per mol Einstein photon adsorbed by HOCl. The lower quantum yield of OCl$^-$ than HOCl (i.e., 0.97 vs 1.45) causes the lower rate of radical formation, resulting in the decrease of NAP degradation (Fang et al. 2014). The second one is that the scavenging rate constant of HO· by OCl$^-$ (8.8×10^9 M^{-1} s^{-1}) is higher than HOCl (2.0×10^9 M^{-1} s^{-1}) (Yang et al. 2014).

Effects of water matrices on the degradation of NAP in UV/chlorine process

The effects of water matrices such as Cl^-, HCO_3^-, and HA on NAP degradation during UV/chlorine process were investigated, and the results are shown in Fig. 4. The NAP degradation in UV/chlorine process was slightly affected by HCO_3^-, the $k_{obs,NAP}$ changed slightly from 0.1751 to 0.1723 min^{-1} with the increase of HCO_3^- concentration from 0 to 50 mM. The HCO_3^- does not participate in the NAP chlorination (Deborde and von Gunten 2008), while it could scavenge reactive radicals $Cl\cdot/OH\cdot$ in UV/chlorine process and forming $CO_3^{\cdot-}$. The negligible effect of HCO_3^- on NAP degradation suggested that the reactivity of $CO_3^{\cdot-}$ with NAP might be close to that of $Cl\cdot/OH\cdot$. In the presence of Cl^- (10~50 mM), the NAP degradation was enhanced. When the concentration of Cl^- increased from 0 to 50 mM, the $k_{obs,NAP}$ gradually increased from 0.1751 to 0.2102 min^{-1}. The Cl^- reacts with $Cl\cdot$ yielding $Cl_2^{\cdot-}$, which might have comparable reactivity with NAP (Wu et al. 2016; Zhu et al. 2018). Notably, the HA (1~5 mg/L) significantly inhibited NAP degradation. This inhibition may result from two reasons. Firstly, HA competed with NAP for chlorine consumption. Secondly, HA could act as UV light filter and scavenger of reactive radicals to reduce constant rate of NAP degradation (Fang et al. 2014).

Degradation pathways of NAP in dark chlorination and UV/chlorine processes

The NAP degradation intermediates at 5, 15, and 30 min in dark chlorination and UV/chlorine processes were detected by HPLC/MS/MS. Figure 5 shows the total ion chromatogram (TIC) of the NAP degradation intermediates at 15 min in UV/chlorine process. The empirical formula (PEF) of intermediates were proposed on the basis of the retention time (t_R) and ratio of mass to charge ($-m/z$) given by TIC. The chemical structure of the product was identified based on the accurate fragmentation spectra of secondary ion mass and previous report. As shown, the NAP (m/z = 230) was determined at t_R of 5.01 min, and the area of NAP decreased with the reaction time. Eleven different intermediates and products were identified at retention times of 1–15 min in UV/chlorine process, and only seven products were detected in chlorination process.

As shown in Fig. 5, all of the intermediates and products were chlorinated-byproducts, suggested that the NAP degradation began with the nucleophilic substitution of naphthalene ring by HOCl, forming Cl-NAP (P1, m/z = 264) (Deborde and von Gunten 2008). Based on the NAP degradation in ozonation, UV photolysis, electro-chemical, and TiO_2-catalytic oxidation processes (Arany et al. 2013; Coria et al. 2016; Chin et al. 2014), it is proposed that NAP degradation in chlorination (dotted lines) and UV/chlorine processes (solid lines) follow three pathways (Fig. 6).

The first pathway briefly termed as demethylation route (R1). The methoxy group of Cl-NAP was attacked by HOCl, yielding phenolic compound P3 (m/z = 250). This was consistent with the formation 2-hydroxyl-1-naphthyl acetone during NAP degradation in chlorination (Kosaka et al. 2016). The propionic acid in fatty chain of P3 was further oxidized by HOCl into ketone intermediate P8 (m/z = 220), which was oxidized into carboxylic product P7 (m/z = 222) (Coria te al. 2016). The carboxylic product (P7) could not be oxidized by HOCl, but could transform into chloro-naphthol compound (P10, m/z = 178) via carboxylic group splitting by UV photolysis (Arany et al. 2013).

The second pathway was described as acetylation route (R2). The propionic acid in fatty chain of Cl-NAP could be attacked by HOCl yielding 6-methoxy-2-acetyl naphthalene (P6, m/z = 234) via acetylation. P6 was an important product during NAP degradation, which was also observed in electro-catalytic oxidation processes (Coria et al. 2016). The methoxy group in P3 was sensitive for HOCl oxidation, forming P8 via $-CH_3$ splitting. The P8 could not only be transformed into P1 via route 1, but also be attacked by reactive chlorine radicals ($Cl\cdot/Cl_2^{\cdot-}$) yielding di-chlorinated intermediate P9 (m/z = 254) (Coria et al. 2016). The acetyl in side-chain of naphthalene ring was broken via direct UV photolysis, finally forming P11 (m/z = 212) (Arany et al. 2013).

The third way termed as decarboxylic route (R3). The HOCl attacked naphthalene ring and methoxy group in side

Table 2 Changes of viciafaba root-tip micronucleus rate by NAP after degradation by chlorination and UV/chlorine processes

Groups	Cell number	Micronucleus cells			MCN	MCI
		Slide 1	Slide 2	Slide 3		
Negative control group	3000	4	3	1	2.67	–
Blank control group	3000	11	15	14	13.33**	4.99
Chlorination group	3000	34	31	26	30.03**	11.25
UV/chlorine group	3000	22	19	26	22.33**	8.36

MCN*, MCN**: significant difference with blank control group (*$p < 0.05$, **$p < 0.01$). Experimental conditions: $I_0 = 0.16$ mW cm^{-2}, $[NAP]_0 = 50$ μM, $[chlorine]_0 = 0.1$ mM, pH = 7.0

chain producing di-chlorinated intermediates P2 ($m/z = 298$) and P4 ($m/z = 284$) via chlorine substitution reaction and de-methylation reaction, respectively. The propionic acid in fatty chain of P4 was decarboxylized into 6-methoxy-2-naphthalene ethylene (P5, $m/z = 238$). The decarboxylic reaction was important pathway during UV photolysis, and P5 was often observed (Arany et al. 2013). Oxidation of ethylene in P5 could further form aldehyde intermediate P9 ($m/z = 254$), which was finally transformed into P11 via split of aldehyde group.

The genetic toxicity variation of NAP during chlorination and UV/chlorine processes

The genetic toxicity variations of NAP during chlorination and UV/chlorine processes were investigated by micronucleus test of Viciafaba tip (Jia et al. 2018). The toxicity of experimental solutions was evaluated by the micronucleus index (MCI), of which higher value suggesting higher genetic toxicity. MCI was estimated according to Eqs. (12) and (13), and the variations of the toxicity are shown in the Table 2. As shown, the micronucleus index MCI of blank groups (only contained NAP) was calculated to be 4.99, indicating that the genetic toxicity of NAP should not be ignored. After chlorination, the MCI increased significantly to 11.25, indicating some of the degradation products processed higher genetic toxicity than NAP. This might be ascribed to the formation of chlorinated-byproducts formation as discussed in section "Degradation pathways of NAP in dark chlorination and UV/chlorine processes". Notably, the MCI of UV/chlorine group was lower (i.e., 8.36) than that of chlorination, indicating that the UV/chlorine process had the potential to reduce genetic toxicity comparing with chlorination.

$$MCN = \frac{Number\ of\ micronucleus\ cells}{Number\ of\ total\ cells} \times 1000 \quad (12)$$

$$MCI = \frac{MCN\ of\ experimental\ group}{MCN\ of\ negative\ control\ group} \quad (13)$$

Conclusions

This study illuminated the NAP degradation efficiencies and pathways in chlorination and UV/chlorine processes. The results demonstrated that chlorination could eliminate NAP efficiently. The combination of chlorine with UV greatly enhanced NAP degradation via generation of reactive radicals. The contributions of chlorination and reactive radicals to the degradation of NAP in UV/chlorine process were calculated to be approximate half to half, and nearly constant at various chlorine dosages. The effects of pH on NAP degradation suggested that chlorination was the dominant way in NAP degradation under acid conditions (pH < 6), while reactive radicals played the leading role under alkaline conditions (pH > 8). The effects of water matrices such as Cl^-, HCO_3^-, and HA on NAP degradation during UV/chlorine process showed that the HCO_3^- (10~50 mM) slightly inhibited, Cl^- (10~50 mM) gradually promoted, and HA (1~5 mg/L) significantly inhibited NAP degradation. The degradation intermediates were detected by HPLC with QE-MS/MS revealing that demethylation, acetylation, and dicarboxylic routes were main degradation pathways during the NAP degradation in UV/chlorine process.

References

Acero JL, Benitez FJ, Real FJ, Roldan G (2010) Kinetics of aqueous chlorination of some pharmaceuticals and their elimination from water matrices. Water Res 44:4158–4170

Alexander SJ (1975) Clinical experience with naproxen in rheumatoid arthritis. Arch Intern Med 135:1429–1435

Arany E, Szabó RK, Apáti L, Alapi T, Ilisz I, Mazellier P, Dombi A, Gajda-Schrantz K (2013) Degradation of naproxen by UV, VUV photolysis and their combination. J Hazard Mater 262:151–157

Bendz D, Paxéus NA, Ginn TR, Loge FJ (2005) Occurrence and fate of pharmaceutically active compounds in the environment, a case study: höje river in Sweden. J Hazard Mater 122:195–204

Boyd GR, Zhang S, Grimm DA (2005) Naproxen removal from water by chlorination and biofilm processes. Water Res 39:668–676

Cai MQ, Feng L, Jiang J, Qi F, Zhang LQ (2013) Reaction kinetics and transformation of antipyrine chlorination with free chlorine. Water Res 47:2830–2842

Cai MQ, Feng L, Zhang LQ (2017) Transformation of aminopyrine in the presence of free available chlorine: kinetics, products, and reaction pathways. Chemosphere 171:625–634

Chin CJM, Chen TY, Lee M, Chang CF, Liu YT, Kuo YT (2014) Effective anodic oxidation of naproxen by platinum nanoparticles coated fto glass. J Hazard Mater 277:110–119

Christen V, Hickmann S, Rechenberg B, Fent K (2010) Highly active human pharmaceuticals in aquatic systems: a concept for their identification based on their mode of action. Aquat Toxicol 96:167–181

Coria G, Sirés I, Brillas E, Nava JL (2016) Influence of the anode material on the degradation of naproxen by Fenton-based electrochemical processes. Chem Eng J 304:817–825

Deborde M, Von Gunten U (2008) Reactions of chlorine with inorganic and organic compounds during water treatment—kinetics and mechanisms: a critical review. Water Res 42:13–51

Deng J, Shao Y, Gao N, Xia S, Tan C, Zhou S, Hu X (2013) Degradation of the antiepileptic drug carbamazepine upon different UV-based advanced oxidation processes in water. Chem Eng J 222:150–158

Dong H, Qiang Z, Hu J, Qu J (2017) Degradation of chloramphenicol by UV/chlorine treatment: kinetics, mechanism and enhanced formation of halonitromethanes. Water Res 121:178–185

Fang J, Fu Y, Shang C (2014) The roles of reactive species in micropollutant degradation in the UV/free chlorine system. Environ Sci Technol 48:1859–1868

Fernández C, González-Doncel M, Pro J, Carbonell G, Tarazona JV (2010) Occurrence of pharmaceutically active compounds in surface waters of the henares-jarama-tajo river system (Madrid, Spain) and a potential risk characterization. Sci Total Environ 408:543–551

Guo ZB, Lin YL, Xu B, Huang H, Zhang TY, Tian FX, Gao NY (2016) Degradation of chlortoluron during uv irradiation and uv/chlorine processes and formation of disinfection by-products in sequential chlorination. Chem Eng J 283:412–419

Hijnen WA, Beerendonk EF, Medema GJ (2006) Inactivation credit of uv radiation for viruses, bacteria and protozoan (oo)cysts in water: a review. Water Res 40:3–22

Jia XH, Feng L, Liu YZ (2018) Degradation behaviors and genetic toxicity variations of pyrazolone pharmaceuticals during chlorine dioxide disinfection process[J]. Chem Eng J 345:156–164

Kosaka K, Nakai T, Hishida Y, Asami M, Ohkubo K, Akiba M (2016) Formation of 2,6-dichloro-1,4-benzoquinone from aromatic compounds after chlorination. Water Res 110:48–55

Luo Y, Guo W, Ngo HH, Nghiem LD, Hai FI, Zhang J, Liang S, Wang XC (2014) A review on the occurrence of micropollutants in the aquatic environment and their fate and removal during wastewater treatment. Sci Total Environ 473-474:619–641

Luo S, Gao L, Wei Z, Spinney R, Dionysiou DD, Hu WP, Chai L, Xiao R (2018) Kinetic and mechanistic aspects of hydroxyl radical–mediated degradation of naproxen and reaction intermediates. Water Res 137:233–241

Morris JC (1966) The acid ionization constant of hocl from 5 to 35°C. J Phys Chem 70:3798–3805

Rosal R, Rodríguez A, Perdigón-Melón JA, Petre A, García-Calvo E, Gómez MJ, Agüera A, Fernández-Alba AR (2010) Occurrence of emerging pollutants in urban wastewater and their removal through biological treatment followed by ozonation. Water Res 44:578–588

Santos JL, Aparicio I, Alonso E, Callejón M (2005) Simultaneous determination of pharmaceutically active compounds in wastewater samples by solid phase extraction and high-performance liquid chromatography with diode array and fluorescence detectors. Anal Chim Acta 550:116–122

Sirés I, Brillas E (2012) Remediation of water pollution caused by pharmaceutical residues based on electrochemical separation and degradation technologies: a review. Environ Int 40:212–229

Štrbac D, Aggelopoulos CA, Štrbac G, Dimitropoulos M, Novaković M, Ivetić T, Yannopoulos SN (2018) Photocatalytic degradation of naproxen and methylene blue: comparison between ZnO, TiO2 and their mixture. Process Saf Environ 113:174–183

Stumpf M, Ternes TA, Wilken RD, Rodrigues SV, Baumann W (1999) Polar drug residues in sewage and natural waters in the state of Rio de Janeiro, Brazil. Sci Total Environ 225:135–141

Tang YQ, Shi XT, Liu YZ, Feng L, Zhang LQ (2018) Degradation of clofibric acid in UV/chlorine disinfection process: kinetics, reactive species contribution and pathways. R Soc Open Sci 5(2):171372

Tixier C, Singer HP, Oellers S, Müller SR (2003) Occurrence and fate of carbamazepine, clofibric acid, diclofenac, ibuprofen, ketoprofen, and naproxen in surface waters. Environ Sci Technol 37:1061–1068

Vieno NM, Härkki H, Tuhkanen T, Kronberg L (2007) Occurrence of pharmaceuticals in river water and their elimination in a pilot-scale drinking water treatment plant. Environ Sci Technol 41:5077–5084

Von Gunten U (2003) Ozonation of drinking water: part ii. Disinfection and by-product formation in presence of bromide, iodide or chlorine. Water Res 37:1469–1487

Wang TX, Margerum DW (2002) Kinetics of reversible chlorine hydrolysis: temperature dependence and general-acid/base-assisted mechanisms. Inorg Chem 33:1050–1055

Watts MJ, Linden KG (2007) Chlorine photolysis and subsequent OH radical production during UV treatment of chlorinated water. Water Res 41:2871–2878

Wu ZH, Fang JY, Xiang YY, Shang C, Li X, Meng FG, Yang X (2016) Roles of reactive chlorine species in trimethoprim degradation in the UV/chlorine process: kinetics and transformation pathways. Water Res 104:272–282

Yang Y, Pignatello JJ, Ma J, Mitch WA (2014) Comparison of halide impacts on the efficiency of contaminant degradation by sulfate and hydroxyl radical-based advanced oxidation processes (AOPs). Environ Sci Technol 48:2344–2351

Zhu YP, Wu M, Gao NY, Chu WH, Li K, Chen S (2018) Degradation of phenacetin by the UV/chlorine advanced oxidation process: kinetics, pathways, and toxicity evaluation. Chem Eng J 335:520–529